Heat Losses from the Receivers of a Multifaceted Parabolic Solar Energy Collecting System

Taebeom Seo*
Department of Mechanical Engineering, Inha University,
253 Younghyundong, Namgu, Inchon 402-751, Korea
Siyoul Ryu
Department of Mechanical Engineering, Graduate School, Inha University,
253 Younghyundong, Namgu, Inchon 402-751, Korea
Yongheock Kang
Renewable Energy Research Department, Korea Institute of Energy Research,
71-2 Jangdong, Yusonggu, Taejeon 305-343, Korea

Heat losses from the receivers of a dish-type solar energy collecting system at the Korea Institute of Energy Research (KIER) are numerically investigated. It is assumed that a number of flat square mirrors are arranged on the parabolic dish structure to serve as a reflector. Two different types of receivers, which have conical and dome shapes, are considered for the system, and several modes of heat losses from the receivers are thoroughly studied. Using the Stine and McDonald model convective heat loss from a receiver is estimated. The Net Radiation Method is used to calculate the radiation heat transfer rate by emission from the inside surface of the cavity receiver to the environment. The Monte-Carlo Method is used to predict the radiation heat transfer rate from the reflector to the receiver. Tracing the photons generated, the reflection loss from the receivers can be estimated. The radiative heat flux distribution produced by a multifaceted parabolic concentrator on the focal plane is estimated using the cone optics method. Also, the solar radiation spillage around the aperture is calculated. Based on the results of the analysis, the performances of two different receivers with multifaceted parabolic solar energy collectors are evaluated.

Key Words: Dish-Type Multifaceted Solar Collector, Receiver, Ray Tracing, Heat Loss

Nomenclature

A_m : Area of a dish concentrator projected on the horizontal plane (m^2)
A_o : Outside surface area of a receiver (m^2)
A_r : Aperture area of a receiver (m^2)
A_w : Heat transfer area inside a receiver (m^2)
d : Aperture diameter of an open cavity (m)
E_{bj} : Blackbody emissive power of cavity sub-region j (W/m^2)
F_{i-j}: View factor from cavity sub-region i to cavity sub-region j
G_{bn}: Solar beam irradiance received as normal incidence on the reflector (W/m^2)
Gr_L: Grashof number based on length L
h : Convective heat transfer coefficient ($W/m^2 \cdot K$)
I : Solar beam intensity ($W/m^2 \cdot sr$)
k_i : Thermal conductivity of the insulator of a receiver ($W/m \cdot K$)
L : Average internal dimension of a cavity (m)
l : Average thickness of the insulator of a receiver (m)
Nu_L: Nusselt number based on length L
T_a : Ambient temperature (K)

* Corresponding Author,
E-mail : seotb@inha.ac.kr
TEL : +82-32-860-7327; **FAX** : +82-32-868-1716
Department of Mechanical Engineering, Inha University, 253 Younghyundong, Namgu, Inchon 402-751, Korea. (Manuscript **Received** October 4, 2002; **Revised** April 28, 2003)

T_w : Surface temperature inside a receiver (K)
δ : Skewness angle from a central ray (rad)
ε_j : Surface radiation emissivity of the cavity sub-region j
η_r : receiver efficiency $\left(=1-\frac{Q_L}{G_{bn}\cdot A_m\cdot \rho_m}\right)$
Ω : Solid angle (sr)
θ : Angle of concentrator/cavity axis to the horizontal surface (rad)
ρ_m : Average reflectivity of a mirror
σ : Scattering parameter (rad)

1. Introduction

A dish-type solar energy collecting system has been developed at the Korea Institute of Energy Research (KIER). The system consists of fifteen parabolically concave circular mirrors which were mounted on the parabolic structure as shown in Fig. 1. In order to develop a more efficient and cheaper system, the system has been modified. One of the most important differences between the first and the second systems is the collector shape. The multifaceted parabolic reflector was considered and a number of flat square mirrors were installed on the parabolic structure as shown in Fig. 2. It was easy to expect that the thermal performance of the second system should be better than that of the first one because the geometric concentration ratio of the second system was much greater than that of the first one. It was also decided that small flat square mirrors would be used as the reflecting element of the parabolic collector. Small mirrors can be manufactured easily and the quality of the back-silver coating of a small mirror is better than that of a large one. Also, it is easy to concentrate the solar energy into the small aperture of the receiver. However, it becomes very difficult to align many mirrors as the number of the mirrors increases. Therefore, the size of the flat square mirrors should be carefully decided in order to optimize thermal performance and assembling difficulty.

In order to obtain the optimal design of a receiver and flat mirrors of a multifaceted reflector, heat losses from a receiver should be thoroughly analyzed. Since convection and radiation

Fig. 1 Parabolic dish type collector at the KIER (Ryu and Seo, 2000)

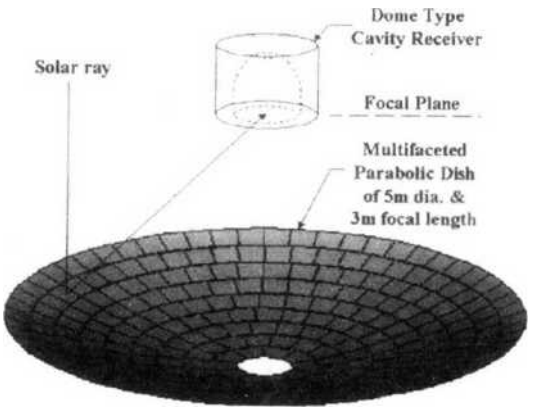

Fig. 2 Multifaceted parabolic dish type collector with 250 mm×250 mm flat mirrors

losses are normally significant compared to conduction loss, convection and radiation heat transfer from a receiver to the surroundings should be carefully investigated. There are several empirical correlations for estimating convection losses for different shapes of cavity type receivers and several working conditions. LeQuere et al. (1981) examined the natural convection losses from two different sized cubical cavities which were similar in shape but different in size. Clausing (1981, 1983) described an analytical model for estimating convection losses from the open cubical cavity receiver. Koenig and Marvin (1981) established an empirically-derived correlation for convection loss from cylindrical cavity type receivers, including the effects of operating temperature and angle. An estimation of

convection losses from a central cylindrical cavity receiver was also performed by Siebers and Kraabel (1984). Improving correlations proposed by Siebers and Kraabel, Stine and McDonald (1989) have suggested an empirical correlation, which has included the effects of the size of a receiver aperture and the receiver tilt angle. However, the estimations by these correlations are not consistent, so we have to be careful when we choose one of these to apply to a particular receiver.

On the other hand, it is difficult to find a simple method for predicting radiation heat transfer from a receiver to its surroundings. Since the major concern for most of the studies was the convection losses, the radiation losses were approximated by a simple equation based on previous research. If the operating temperature is low, however, the convection losses are also relatively low compared with those for receivers working at high temperatures where the radiation losses become significant. In particular, multifaceted solar energy concentrator is somewhat different from a full-surface concentrator. Because the characteristics of solar irradiation entering the receivers change as the size of the mirror changes, it is difficult to use the design information that has been reported for other systems. For example, the multifaceted reflector at White Cliffs in Australia which has about 2300 flat square mirrors of 100 mm×100 mm (Kaushika, 1993), has been reported. However, useful design information for the second system which is being designed at KIER is unavailable.

Therefore, in the present study heat losses from the receivers with the multifaceted reflector are estimated and their thermal performances are investigated to find the optimal design of both the receiver and the mirrors for multifaceted solar thermal system. Five different sizes of the mirror element and two different types of receivers are considered. Based on the calculations, each mode of heat loss and the thermal performance of two receivers are compared at several different operating temperatures and mirror sizes. Summarizing the output of the calculation, optimal sizes of the mirror and the receiver can be suggested.

2. Modeling of Heat Losses

2.1 Solar irradiation

Based on the definition of radiation intensity, heat flux by solar irradiation at a random point is

$$q=\iint I\cos\phi\, d\Omega \tag{1}$$

The intensity distribution of the cone ray of solar irradiation is called a 'sunshape' and can be expressed as a Gaussian Function (Jeter, 1986).

$$f=\frac{I}{G_{bn}}=\frac{R}{2\pi\sigma^2}\exp\left(-\frac{\delta^2}{2\sigma^2}\right) \text{ when } \delta\le n\sigma \qquad =0 \text{ when } \delta>n\sigma \tag{2}$$

where R is equal to $\rho_m/(1-\exp(-n^2/2))$. Hence, the concentration ratio can be obtained by integrating Eq. (2) twice with respect to the solid angle (Jeter, 1986).

$$Cr=\frac{q}{G_{bn}}=\iint f\cos\phi\, d\Omega \tag{3}$$

The concentration ratio at any point and the heat flux distribution can be found from Eq. (3) on a focal plane. From the flux distribution, the total solar irradiation entering a receiver is calculated as :

$$Q_{IN}=G_{bn}\times\int_{Ar} Cr\, dA_r \tag{4}$$

2.2 Heat losses from receivers

Heat losses from a receiver occur due to the temperature difference between the receiver and its surroundings and depend on the geometry of the receiver and the collector. In order to optimally design the receiver, it is important to predict the amount of heat loss from the receiver.

In this study, heat losses from the receivers are classified as

① spillage loss of solar energy reflected by a collector around a receiver.

② conductive loss through the insulating materials.

③ convective loss through the receiver aperture.

④ radiative loss by surface emission from the inner surface of the receiver.

⑤ radiative loss by reflection off the inner surface of the receiver.

In general, spillage loss can occur due to several reasons. In this study, only spillage loss due to the size of the flat square mirror and the geometry of the receiver is considered. The amount of spillage loss around the aperture can be calculated as

$$Q_{OUT}=G_{bn}\cdot A_m\cdot \rho_m - Q_{IN} \tag{5}$$

In order to evaluate the conductive loss from receivers, the following equation (Kaushika, 1993) is used.

$$Q_{COND}=\frac{1}{\frac{1}{A_o h}+\frac{l}{k_i\sqrt{A_o A_w}}}(T_w-T_a) \tag{6}$$

The average convective heat transfer coefficient, h, on the external surface of a receiver is evaluated from an empirical correlation for external flow around a cylinder proposed by Hilpert (1933). Because the shadow of the receiver on the concentrator reduces the amount of solar irradiation entering the receiver, increasing the insulation thickness of the receiver is not recommended. Hence, an optimal insulation thickness exists for each system. However, we do not need to consider the shading effect in this study because there is no reflecting surface at the center of the parabolic structure of the KIER system shown in Fig. 2.

Convective heat transfer from the aperture of a receiver is difficult to analyze because there are many factors affecting convective heat transfer. Convection loss depends on, for example, the shape of the receiver, the speed and direction of the wind, and the working temperature. Several empirical correlations have been suggested. As most of them were developed for the specific shape and operating conditions of a particular receiver, it was difficult to find a general correlation applicable to many different types of receivers with any reasonable accuracy. Therefore, the appropriate correlation for a particular receiver should be carefully selected in order to predict the convection loss accurately.

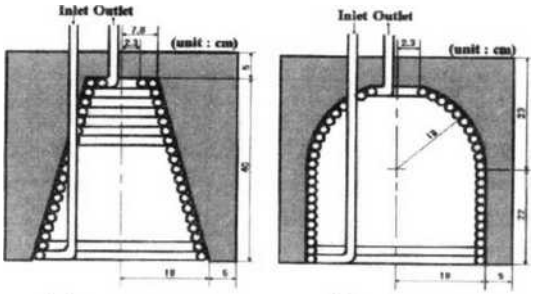

(a) Conical type (b) Dome type

Fig. 3 Geometry of receivers (Ryu and Seo, 2000)

In order to select the best convective loss model for the KIER receivers, several models were applied to the receiver developed for the Solar Total Energy Project (STEP) (McDonald, 1995), which was very similar to that for the KIER system shown in Fig. 3. From the results of Ryu and Seo(2000) it is clear that the Clausing model and the Stine and McDonald model can predict the convection loss from the STEP receiver more accurately than others. The Clausing model is inconvenient to use because it is implicit unlike the Stine and Mcdonald model. From this reason, the convection loss for the present study is estimated using the Stine and Mcdonald model.

Improving correlation as proposed by Siebers and Kraabel (1984), Stine and McDonald have suggested the following empirical correlation, which includes the effects of the size of the receiver aperture and the receiver angle.

$$Nu_L=0.088Gr_L^{1/3}\left(\frac{T_w}{T_a}\right)^{0.18}(\cos\theta)^{2.47}\left(\frac{d}{L}\right)^{s} \tag{7}$$

where s is $1.12-0.98d/L$. From this equation, the average convective heat transfer coefficient on the inner surface of a receiver can be obtained and the total losses by convection heat transfer can be calculated using the Newton's Cooling Law, $q=h\Delta T$.

Radiation losses from a receiver can be classified into two categories. One is surface emission from the inner surface of the receiver to its surroundings, which is called emission loss. The other is reflected solar irradiation off the inner surface that escapes from the receiver. In other

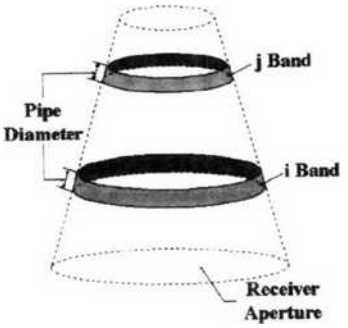

Fig. 4 Conceptual diagram for the Net Radiation Method (Ryu and Seo, 2000)

words, solar irradiation is reflected by the concentrator first. After being focused at the receiver, solar irradiation hits the inner surface of the receiver. Although it depends on the radiation property of the inner surface, most of the energy is absorbed by the surface. Unfortunately, a certain amount of solar energy that enters the receiver escapes from the receiver by surface reflecting. This is called reflection loss in the present study. The Net Radiation (Dehghan and Behnia, 1996; Modest, 1993) and the Monte-Carlo (Yang et al., 1995) methods are used to evaluate emission and reflection losses, respectively.

For the Net Radiation Analysis, the inner surface of the receiver is divided into a number of small bands as shown in Fig. 4. Assuming that the inner surface of a receiver is diffuse and gray, radiation heat exchange between each band can be expressed as the following equation indicating the energy balance on each surface of the bands (Dehghan and Behnia, 1996).

$$\sum_{j=1}^{n}\left[\frac{\delta_{ij}}{\varepsilon_j}-\left(\frac{1}{\varepsilon_j}-1\right)F_{i-j}\right]q_j=\sum_{j=1}^{n}[\delta_{ij}-F_{i-j}]E_{bj} \quad (8)$$

Therefore, if the temperature, the emissivity, and the view factors are known for each band in a receiver, it is easy to calculate the radiation heat transfer rate in each band using Eq. (8). It is supposed that the temperature distribution inside a receiver has a linear variation from the inlet to the exit. The view factors between the bands are obtained from the ready-made formulas for similar geometries and the reciprocity of the view factor (Modest, 1993). The radiation loss from the cavity represents the heat transfer rate from the artificial surface that coincides with the aperture plane.

In order to estimate the amount of escaping solar energy reflected by the inner surface, the statistical ray tracing method, called the Monte-Carlo method, is used for this study. For the analysis, it is assumed that a solar ray is specularly reflected on the surface of the mirror, and then it is diffusely reflected on the inner surface of the receiver (Ryu and Seo, 2000). Otherwise, it is absorbed into the inner surface of the receiver. Furthermore, the radiation properties are assumed to be independent of the wave number. The parabolic structure holding the mirrors is assumed to face the sun at all times during the operation. Because the receiver is made of a long circular tube, the inner surface is wavy and the shape of each wave is a half circle. However, the inner surface is assumed to be flat for the simplicity of the calculation. If we consider the real wavy surface, it is too complicated to trace the photon bundle. In order to begin the ray tracing procedure, an artificial photon bundle is numerically generated toward the parabolic structure. The direction of the photon bundle generated is parallel to that of a solar ray coming directly from the sun to the collector. Diffuse radiation, which is not important from the heat transfer point of view, is not considered here. Whenever the photon bundle hits the surface, it is statistically determined whether it is absorbed or reflected using the radiation properties of the surface. If the total number of photon bundle absorbed into the inner surface of the receiver is N_a among N of photon bundles entering the receiver aperture, the value of radiation loss by the inner surface reflection of the receiver is calculated as follows.

$$Q_{RAD}=Q_{IN}\frac{N-N_a}{N} \quad (11)$$

While the amount of radiative heat transfer is accurately calculated by the Monte-Carlo method, the solution changes depending on the number of photon bundles generated because it is a statistical approach. Fig. 5 shows the apparent reflectivity $((N-N_a)/N\times 100)$ of the conical

receiver shown in Fig. 3(a) as the number of photon bundles generated in a 100 mm by 100 mm multifaceted parabolic reflector changes. As shown in this figure, if more than 2.5 million photon bundles are generated on a reflector, the deviation becomes less than 0.8%. In this study, the apparent reflectivities of the receivers are determined using 3 to 6 million photon bundles which are numerically generated.

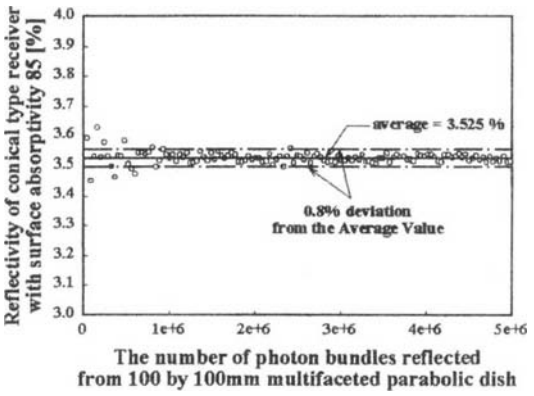

Fig. 5 Convergence of the Monte Carlo method for 100 mm by 100 mm facets and the conical receiver (surface reflectivity of the receiver= 0.85)

3. System Configurations and Working Conditions

It is assumed that the reflector consists of a number of flat square mirrors as shown in Fig. 2. The focal length and the rim angle of the parabolic structure are 3 m and 45°, respectively, which are the same as the previous system, shown in Fig. 1. Five different flat square mirrors, of which length of the side are 100, 150, 200, 250, 300 mm, are considered, and their thermal performances are calculated and compared. Table 1 summarizes the specifications of the reflectors. The geometrical concentration ratio (A_m/A_r) of the multifaceted reflector is about 67%~70% larger than the previous one because the empty space of the multifaceted reflector is smaller than that of the previous system.

The conical and dome receivers shown in Fig. 3 are investigated. The aperture radii of both receivers are 180 mm, and the diameter and height

Table 1 Summary of reflecting surfaces

	Mirror type	Number of mirrors	Projected area of mirrors (m^2)	Geometric Cr (A_m/A_r)
Previous system	Parabolic dish of 1 m dia. and 3 m focal length	15	11.33	111.3
Multifaceted reflector	100 mm×100 mm flat mirrors	2038	19.28	189.4
	150 mm×150 mm flat mirrors	904	19.18	188.4
	200 mm×200 mm flat mirrors	510	19.09	187.5
	250 mm×250 mm flat mirrors	326	18.98	186.5
	300 mm×300 mm flat mirrors	227	18.87	185.4

Table 2 The nominal operating conditions for the system

mirrors	Reflectivity	0.85
Receiver	Thermal conductivity of the insulator (glass fiber)	0.046 W/mK
	Absorptivity of the inner surfaces	0.85
Solar input	Solar beam irradiance received for normal incidence on the reflectors	800 W/m^2
	Standard deviation of Gaussian distribution (σ)	0.267°
Weather	Ambient temperature	25℃
	Wind velocity	3.5 m/s

of the receivers are 460 mm and 450 mm, respectively. The inner surface areas are 0.35 m^2 in the conical receiver and 0.45 m^2 in the dome receiver. The inner surface area of the dome receiver is about 29% larger than that of the conical one.

In Table 2, the nominal conditions for the calculation are summarized. The data are chosen in order to simulate typical Korean weather conditions.

4. Results and Discussion

Fig. 6 shows the distribution of the concentration ratio at the focal plane. The concentration ratio at the center of the focal plane reaches its maximum when the size of the mirror is 100 mm $\times$100 mm. The maximum concentration ratio at the center is 1445, and then rapidly decreases as the radial distance increases. The concentration ratio becomes zero if it is about 110 mm away from the center of the focal plane. The distribution of the concentration ratio for different sizes of mirrors shows that the solar irradiation reflected from the mirrors does not concentrate well as the size of the mirror increases. The concentration ratio of the 300 mm $\times$300 mm mirror at the radial distance of 150 mm is 160 and the shape of distribution is flat. When the 200 mm $\times$200 mm mirror is used and the aperture of the receiver is 180 mm, a small amount of solar energy spillage around the aperture occurs. The amount of spillage greatly increases with the size of the mirror.

The apparent reflectivities of the receivers are compared in Table 3. The apparent reflectivities of the dome receiver are lower than those of the conical one. It is because the inner surface area of the dome receiver is 29% larger than that of the conical one, which gives more chances to absorb the reflected photons. The apparent reflectivities of both receivers increase with the size of the mirror. If the size of the mirror increases, the number of photons which hit the inner surface of the receiver near the aperture increase. Considering that the view factor of the vicinity of the receiver entrance to the aperture is relatively large compared with that of the area deep inside of the receiver, it can be said that the trend of the data presented in the table is physically reasonable.

In Table 4, heat losses from the receiver with 200 mm $\times$200 mm mirrors are summarized. Those data are plotted in Fig. 7. The conductive and the spillage losses are relatively small so that their effects on the thermal performance of the system are negligible. In Fig. 7(a) the reflection loss of the conical receiver is greater than the other modes of heat losses. In addition, the value is much larger than that for the previous system, which is 282 W (Ryu and Seo, 2000). This is because the apparent reflectivity and solar energy input to the receiver of the present system increase significantly. The apparent reflectivity of the conical receiver for the previous system is 3.660% (Ryu and Seo, 2000) and that for the present system is 4.066%. The amounts of solar energy entering the receivers for the previous and present systems are 7.7 kW and 12.9 kW, respectively. The amount of reflection loss does not depend upon the working temperature because the radiation

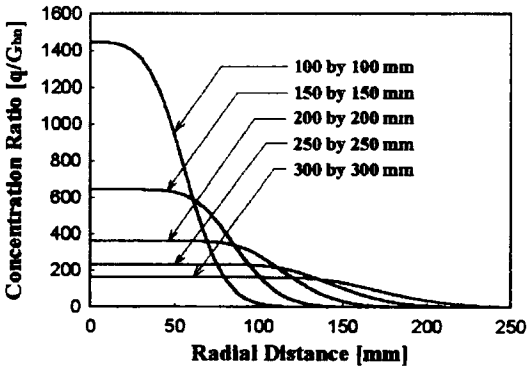

Fig. 6 The distribution of the local concentration ratio on the focal plane for a solar half angle 0.267°

Table 3 The apparent reflectivity $((N-N_a)/N\times 100)$ of the receivers

	Conical receiver (%)	Dome receiver (%)
100 mm $\times$ 100 mm mirror	3.525	2.871
150 mm $\times$ 100 mm mirror	3.743	2.993
200 mm $\times$ 100 mm mirror	4.066	3.185
250 mm $\times$ 100 mm mirror	4.503	3.465
300 mm $\times$ 100 mm mirror	4.804	3.624

Table 4 Heat losses from the receivers with 200 mm×200 mm mirror

Receiver type	Working Temp. (℃)	Spillage loss (W)	Conductive loss (W)	Convective loss (W)	Radiative losses (W)		Total loss (W)
					Emission	Reflection	
Conical	100	12	17	62	52	527	670
	125	12	23	92	73	527	727
	150	12	29	126	99	527	793
	175	12	35	162	130	527	866
	200	12	41	201	166	527	947
Dome	100	12	28	80	70	413	603
	125	12	38	119	100	413	682
	150	12	47	162	137	413	771
	175	12	57	209	182	413	873
	200	12	66	259	236	413	986

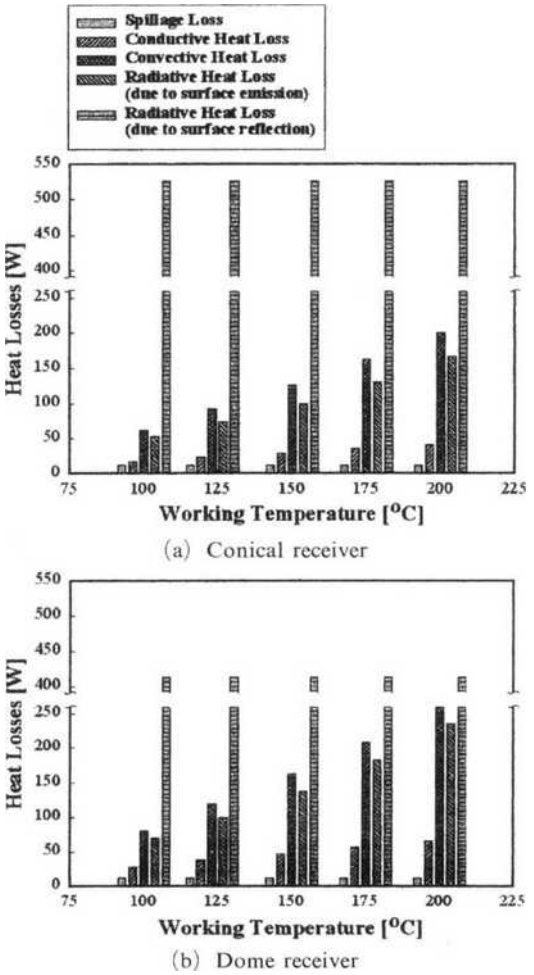

Fig. 7 Heat losses from receivers with 200 mm×200 mm mirrors

properties of the inner surface of the receivers are assumed to be independent of the temperature. Therefore, the reflection loss becomes a function of shape. The convection and emission losses increase with the working temperature. The total loss reaches 947 W at a working temperature of 200℃. Heat losses from the dome receiver are shown in Fig. 7(b). Since the inner surface area of the dome receiver is larger than that of the conical receiver, convection and emission losses increase by 29.0% and 38.4%, respectively, while the reflection loss decreases by 21.6%. According to Table 4, the total loss of the conical and the dome receivers changes from 670 W to 947 W and from 603 W to 986 W, respectively, as the working temperature increases. Therefore, it is known that the dome receiver is good for lower working temperatures while the conical receiver is appropriate for higher working temperatures. In addition, reflection loss becomes important as the working temperatures decrease.

Fig. 8 shows spillage and reflection losses from both conical and dome receivers as the size of the mirrors increases. Conduction, convection, and emission losses are independent of the size of the mirrors so these are not shown in the figure. Since spillage loss depends only on the size of the aperture, there is no difference between the two receivers. Spillage loss is zero and negligible if the size of the mirror is smaller than 200 mm×200 mm. This is the reason why the 200 mm×200 mm

mirror is chosen for the data presentation of the study. If the mirror is larger than 200 mm×200 mm, spillage loss increases rapidly. On the other hand, reflection losses increase gradually as the size of the mirror increases. Once the size of the mirror is larger than 250 mm×250 mm, reflection loss decreases because the total energy input decreases due to the significant increase of spillage loss.

The efficiency and the heat capacity of the receivers are shown in Fig. 9. Heat capacity refers to the amount of solar energy transferred to the working fluid. The differences of the efficiencies and the heat capacities for two kinds of receivers are not great. On the other hand, the efficiency and the heat capacity of the receiver significantly depend on the working temperature and the size of the mirrors. The efficiency of the dome receiver at a working temperature of 100℃ is better than that of the conical receiver, while the conical receiver is better at a working temperature of 200℃. When the working temperature is 100℃ and the size of the mirror is 100 mm×100 mm, the efficiencies are about 95.6% and the heat capacity is about 12.5 kW. The efficiency and heat capacity decrease gradually as the size of the mirror increases. Once the size of a mirror is greater than 200 mm×200 mm, the efficiency and the heat capacity rapidly drop to 81.8% and 10.5 kW, respectively, because of the significant increase of spillage loss. At a working temperature of 200℃, the efficiency and heat capacity of the receiver are 93.1% and 12.2 kW if the size of the mirror is 100 mm×100 mm.

Figure. 10 shows a graphical comparison of receiver efficiency and thermal capacity depending on working temperatures in both the existing KIER system and the 200 mm by 200 mm multifaceted concentrator. The 200 mm by 200 mm facet reflector shows superior performance in general to the existing KIER reflector, which is because 200 mm by 200 mm mirrors have about a 68% larger area projected on the horizontal plane; this concentrates much solar irradiation, and makes for a small spillage loss. At a working temperature of 100℃, the dome receiver has about 0.8% larger efficiency than the existing system, making for a difference up to about 3.1% greater with the increase in temperature. In addition, the thermal capacity improved about 71.6% over the

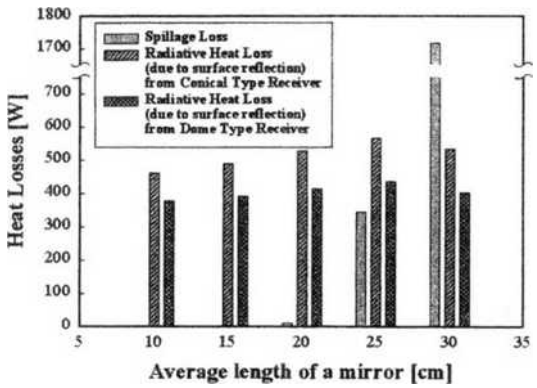

Fig. 8 Spillage loss and reflection loss from the receivers for different sizes of mirrors

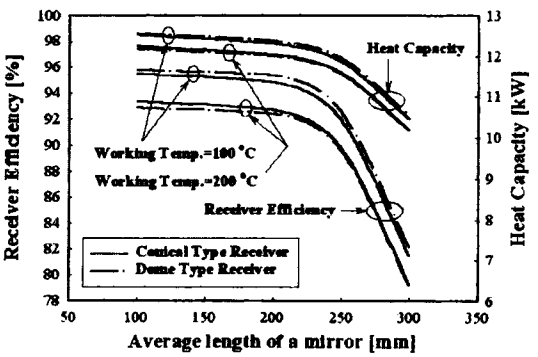

Fig. 9 Thermal efficiency and heat capacity for conical and dome type receivers

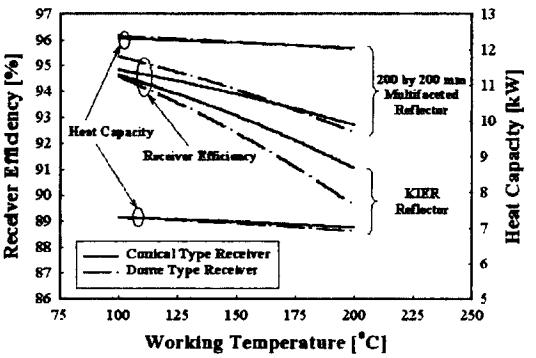

Fig. 10 Comparison of thermal efficiency for KIER reflector and 200 mm by 200 mm multifaceted parabolic reflector systems

existing system. The conical receiver showed a maximum increase of 1.8% and 71.5% respectively in efficiency and heat capacity compared to the previous system.

5. Conclusions

According to this study, when the shape of a reflector is changed to that of a multifaceted parabolic dish as in the existing KIER solar energy concentrating system, the prediction for heat loss in both conical and dome receivers concludes as follows:

(1) The distribution of heat flux around the receiver aperture is greatly affected by the size of the mirrors in the reflector, and if the size exceeds 200 mm by 200 mm, solar irradiation escaping out of the receiver rapidly increases.

(2) The investigation into receiver efficiency and thermal capacity proved that mirrors of 200 mm by 200 mm showed relatively good performance without great heat loss. In both receivers, efficiency and thermal capacity began to decrease from 95.1% and 12.3 kW, respectively, at lower temperatures to about 92.5% and 12.0 kW, as the temperature increased.

(3) The examination of the total heat loss for various shapes of a receiver with 200 mm by 200 mm mirrors revealed that the dome receiver is beneficial at lower temperatures while the conical receiver has better performance at higher temperatures.

(4) The comparison of the existing KIER system and the 200 mm by 200 mm multifaceted concentrator showed that receiver efficiency increased 0.8~3.1% in the dome receiver and 0.2~1.8% in the conical receiver depending on the working temperatures, when compared to the present system. On the other hand, thermal capacity increased 70% on average.

(5) In this study, the most ideal data were used for the distribution of radiation intensity reflected from the mirrors. However, if empirical data on the tracking errors of a concentrator and the surface errors of a reflector are collected, more accurate predictions would be possible.

References

Clausing, A. M., 1981, "An Analysis of Convective Losses from Cavity Solar Central Receivers," *Solar Energy*, Vol. 27, No. 4, pp. 295~300.

Clausing, A. M., 1983, "Convective Losses from Cavity Solar Receivers-Comparisons between Analytical Predictions and Experimental Results," *ASME Journal of Solar Energy Engineering*, Vol. 105, pp. 29~32.

Dehghan, A. A. and Behnia, M., 1996, "Combined Natural Convection-Conduction and Radiation Heat Transfer in a Discretely Heated Open Cavity," *ASME Journal of Heat Transfer*, Vol. 118, pp. 56~64.

Incropera, F. P. and DeWitt, D. P., 1996, *Fundamentals of Heat and Mass Transfer*, 4th Edn. Wiley, p. 368~371.

Jeter, S. M., 1986, "The Distribution of Concentrated Solar Radiation in Paraboloidal Collectors," *ASME Journal of Solar Energy Engineering*, Vol. 108, pp. 219~225.

Kaushika, N. D., 1993, "Viability Aspects of Paraboloidal Dish Solar Collector Systems," *Renewable Energy*, Vol. 3, No. 6/7, pp. 787~793.

Koenig, A. A. and Marvin, M., 1981, "Convection Heat Loss Sensitivity in Open Cavity Solar Receivers," Final Report, DOE Contract No. EG77-C-04-3985.

LeQuere, P., Penot, F. and Mirenayat, M., 1981, "Experimental Study of Heat Loss through Natural Convection from an Isothermal Cubic Cavity," *Sandia National Laboratories Report*, SAND81-8014, pp. 165~174.

McDonald, C. G., 1995, "Heat Loss from an Open Cavity," *Sandia National Laboratories Report*, SAND95-2939.

Modest, M. F., 1993, *Radiative Heat Transfer*, McGraw Hill, pp. 193~209.

Ryu, S. Y. and Seo, T. B., 2000, "Estimation of Heat Losses from the Receivers for Solar Energy Collecting System of Korea Institute of Energy Research," *Journal of Korea Society of Mechanical Engineers*, Vol. 14, No. 11, pp. 1403~1411.

Siebers, D. L. and Kraabel, J. S., 1984, "Estimating Convective Energy Losses from Solar

Central Receivers," *Sandia National Laboratories Report*, SAND84-8717.

Stine, W. B. and McDonald, C. G., 1989, "Cavity Receiver Convective Heat Loss," *Proceeding of the International Solar Energy Society Solar World Congress*, Kobe, Japan, pp. 1318~1322.

Yang, W. J. et al., 1995, *Advances in Heat Transfer*, Vol. 27, Academic Press.